Applied Physics B (2024) 130:72
https://doi.org/10.1007/s00340-024-08216-x

Applied Physics B
Lasers and Optics

RESEARCH

Atomic versus molecular plasmas for frequency conversion of laser radiation: stronger harmonics, larger cutoffs, better stability, resonance, and quasi-phase-matching enhancement

Rashid A. Ganeev[1,2] · Bakhadir S. Mirzaev[1]

Received: 1 December 2023 / Accepted: 2 April 2024 / Published online: 12 April 2024

Abstract
High-order harmonic generation in laser-induced plasmas is analyzed from the point of view of presence of either molecular or atomic components. Comparison of boron carbide, carbon, and boron plasmas demonstrates the worsened characteristics of coherent extreme ultraviolet radiation in the case of B_4C (smaller conversion efficiency, lower cutoff of generated harmonics, worsened stability). Similar features, alongside the disappearance of resonance-induced enhancement of harmonics and weakened quasi-phase-matching conditions, were observed in other molecular plasmas (Ag_2S, GaAs, Cr_3C_2) compared with plasmas comprising atomic components (Ag, As, Cr). We discuss the reasons of worsening conditions in the case of high-order harmonic generation in few-atomic molecular species compared to the single-atomic ones.

1 Introduction

High-order harmonic generation (HHG) in laser-induced plasmas (LIP) allows for the formation of coherent extreme ultraviolet (XUV) sources in the wavelength region of 8–100 nm. This technique was developed in the nineties [1–6] and has shown new opportunities in the enhancement of the conversion efficiency using different mechanisms (resonance-induced enhancement of single harmonic, nanoparticles-induced enhancement of whole set of harmonics, quasi-phase matching (QPM) of a tunable group of harmonics in XUV, two-color pump (TCP)). QPM and TCP have been earlier demonstrated in the case of HHG in gases [7–17], while resonance-induced enhancement of single harmonic and nanoparticle-induced enhancement of a whole set of harmonics are mostly attributed to the advanced features of HHG in LIP. The processes of harmonic enhancement in LIP were frequently analyzed in numerous laboratories worldwide [18–43].

The application of almost all non-radioactive solid elements of the periodic table allowed determining the most attractive of them from the point of view of strongest harmonics in different spectral ranges (Ag, C) and extended cutoff (Mn, V). While applying the above-mentioned methods, most of the advanced results during HHG using LIP were obtained in the case of the atomic plasmas [44–46]. The free electrons being presented in LIP prevent maintenance of the phase-matching between the fundamental and harmonics waves [15, 17]. Correspondingly, one has to avoid large concentration of those species in LIP when choosing the fluence of heating pulses during ablation of targets and formation of optimal plasma. Meanwhile, small fluencies of heating pulses do not allow formation of the plasmas comprising large number of single-atomic particles, which also restricts HHG conversion efficiency. The optimization of ablation conditions for each case of atomic targets allows for generation of the largest yield of harmonics.

Meanwhile, the molecular species represent a majority of materials available for HHG in gases and laser-induced plasmas. Initially, the simplest gaseous molecules like nitrogen, oxygen, nitrogen oxide, chlorine, etc. were applied as the media for HHG during propagation of strong femtosecond pulses through the gas jets and cells [47–49]. It was predicted that nuclear dynamics can reduce the emission intensity from NO and NO_2 molecules by more than 50% compared to the atomic species [47]. The comparison with single-atomic noble gases has shown the limitations in the

✉ Rashid A. Ganeev
rashid_ganeev@mail.ru

[1] TIIAME National Research University, Kori Niyoziy 39, 100000 Tashkent, Uzbekistan

[2] Department of Optics and Spectroscopy, Voronezh State University, Voronezh 394006, Russia

HHG conversion efficiency and harmonic cutoffs using the molecular gases. Strong laser field ionization of molecules and HHG from molecules has been studied in [49]. It was underlined that the mechanism of observed ionization suppression of some molecules is still under debate. It was found that there are strong correlations between ionization suppression and extension of harmonic cutoff. By carefully examining the harmonic spectra near the cutoff region, the authors of Ref. [49] underlined the role of the alignment of molecules in the process of harmonic generation.

First attempts in using molecular targets for the formation of LIP and HHG also did not show the advantages compared with the atomic targets [3, 6]. The optimization of LIP formation in that case also did not result in the improvement of the intensity and cutoff of generating emission. Among the reasons leading to the worsening of HHG in these media compared with atomic plasmas could be (a) the growing concentration of free electrons, which caused the phase mismatch, (b) the increase of the incoherent plasma emission in XUV region, which restricts the observation of harmonic emission at the conditions of stronger ablation of targets, (c) alignment of molecules, and (d) ionization suppression.

In the present study, the comparison of HHG in the plasmas containing molecules and atoms is presented. The aim of these studies was to show a difference in HHG efficiency between the plasmas containing atoms and molecules. Because of this we chosen the pairs of plasmas containing similar atoms (Ag_2S and Ag, GaAs and As, Cr_3C_2 and Cr, B_4C and C). These plasmas were systematically analyzed and the most important results are reported. Particularly, the comparison of the boron carbide, carbon, and boron plasmas demonstrated the worsened characteristics of coherent XUV radiation in the case of B_4C LIP (weaker conversion efficiency, lower order of generating harmonics, insufficient stability). Similar features were observed in other few-atomic molecular plasmas once compared with atomic components. Additionally, in most cases, the molecular plasmas did not allow the resonance-induced enhancement of single harmonic and QPM-induced enhancement of a group of harmonics compared with the atomic plasmas. The reasons in worsening of the conditions of HHG in multi-atomic species compared with single-atomic ones are discussed.

2 Results and discussion

The standard technique of HHG in LIPs was used [45]. The focused picosecond radiation (800 nm, 250 ps, 2 mJ, 10 Hz) at the fluencies varying in a broad range (0.7–3 J cm^{-2}) was used for ablation of the targets placed in the vacuum chamber (Fig. 1). Various targets were inserted on the translating stage allowing optimization of their position with regard to the focal position of the driving pulses. Those included the

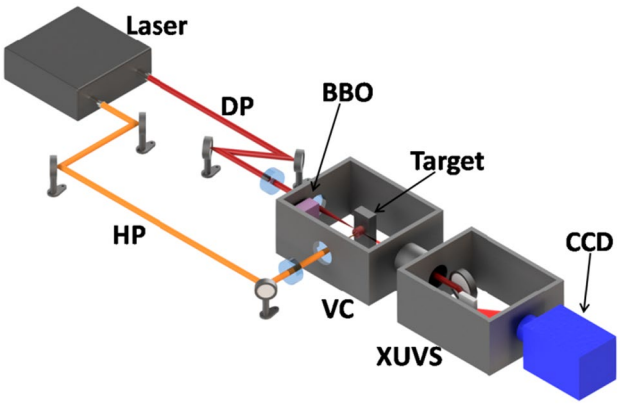

Fig. 1 Experimental scheme describing HHG in LIPs. Laser: Ti: sapphire laser and optical parametric amplifier providing the picosecond and femtosecond pulses. *DP* driving pulses, *HP* heating pulses, *BBO* barium borate crystal for generation of the second harmonic of driving pulses. Target: various targets installed in the translating stage. *VC* vacuum chamber, *XUVS* extreme ultraviolet spectrometer, *CCD* charge-coupled device camera for registering the spectral distribution of harmonics detected by micro-channel plate

atomic (B, C, Ag, As, Cr) and molecular (B_4C, Ag_2S, Cr_3C_2, GaAs) species.

The femtosecond driving radiation (800 nm, 65 fs, 4 mJ, 10 Hz or 1200–1500 nm, 70 fs, 1 mJ, 10 Hz) was used for harmonic generation in the molecular and atomic LIPs. This radiation was focused inside the formed plasmas at a distance of 0.3 mm from the target surface. The delay between heating and driving pulses was maintained at the conditions corresponding to the maximal harmonic yield for each LIP. It varied between 60 and 200 ns depending on the used target. The heavier targets required longer delays between the heating and driving pulses to form the maximal concentration of particles along the path of the driving pulses.

The plasma and harmonic emissions were analyzed by a hand-made XUV spectrometer contained a cylindrical mirror and a 1200 grooves/mm flat field grating (FFG 124, Hitachi Photonics) with variable line spacing. The spectrum was recorded by a micro-channel plate (MCP, Hamamatsu) detector with the phosphor screen, which was imaged onto a CCD camera. The integration time of CCD camera (1 s for the 10 Hz pulse repetition rate laser) was the same for the whole set of experiments. Thus the spectral images of harmonics, either raw spectra or their plots, can be compared with each other since the collection of harmonic spectra images was identical for all groups of experiments. The movement of MCP along the focusing plane of FFG allowed observation of harmonics in different regions of XUV.

2.1 Comparison of HHG in carbon, boron, and boron carbide LIP: decreased harmonic yield and cutoff from the molecular plasma

The low-order harmonic generation in boron carbide plasma is sensitive to the presence of atoms, molecules, clusters, and nanoparticles in a LIP, and can, in some cases, be used as a probe of their density [50–52]. The main goal of the present studies was a comparison of the harmonic yield from the plasmas containing molecular structure (B_4C) and atoms (B and C) at the best conditions of plasma formation and similar intensity of the driving pulses (2×10^{14} W cm^{-2}). Notice that all studies were carried out in a single set of measurements and using similar conditions of registration of harmonic emission. For each of those plasmas, the maximal yields of harmonics were compared. As one can see, the weak harmonics up to the 23rd order (H23) of 800 nm radiation were observed from the B_4C plasma (Fig. 2a). Then two atomic plasmas (boron and carbon) were analyzed. Below, we show the comparative disadvantages of B_4C LIP compared to the B LIP and C LIP.

Figure 2b shows the spectral distribution of harmonics from carbon plasma at similar ablation conditions as in the case of B_4C plasma. Both yield and harmonic cutoff were improved in the case of the carbon plasma. The maximally generated order of harmonics was increased to H27 and the enhancement factor of harmonics in the range of H15–H23 was varied in the range between 3x (for H15) and 12x (for H23). Boron plasma showed a significant difference in harmonic cutoff and distribution once compared with B_4C LIP (Fig. 2c). The harmonics starting from H17 (not shown in Fig. 2c) demonstrated a plateau-like shape until H51, while the cutoff was at H57. H23 shown in Fig. 2c was almost 15 times stronger than the same harmonic in the case of the boron carbide plasma.

These measurements were carried out using the titanium sapphire laser operated at $\lambda = 800$ nm. The comparative studies showed influence of the composition of the plasmas produced in three studied cases on the spectral distribution and intensity of harmonics. In the case of B_4C plasma, the growth of the fluence of heating pulses above some threshold level led to an increase in free electron concentration leading to the phase mismatch between driving pulses and higher-order harmonics. The additional disadvantage in the growth of the fluence of heating pulses above the "optimal" level is an appearance of incoherent emission of plasma in the XUV region, which became significantly stronger than the emission of harmonics. The emission of B_4C plasma comprised the transitions of the single and double-charged B and C particles, which was not observed in the case of two other targets at the optimal conditions of ablation. Correspondingly, the ablation of C and B targets at these conditions did not lead to a decrease in harmonic cutoff and harmonic yield.

Similar features of harmonics from B_4C and C plasmas were observed in the case of driving pulses from the optical parametric amplifier ($\lambda = 1420$ nm). The experiments were performed using TCP of boron carbide and carbon LIP at the conditions when the installation of a thin (0.3 mm) barium borate (BBO) crystal on the path of the driving 1420 nm

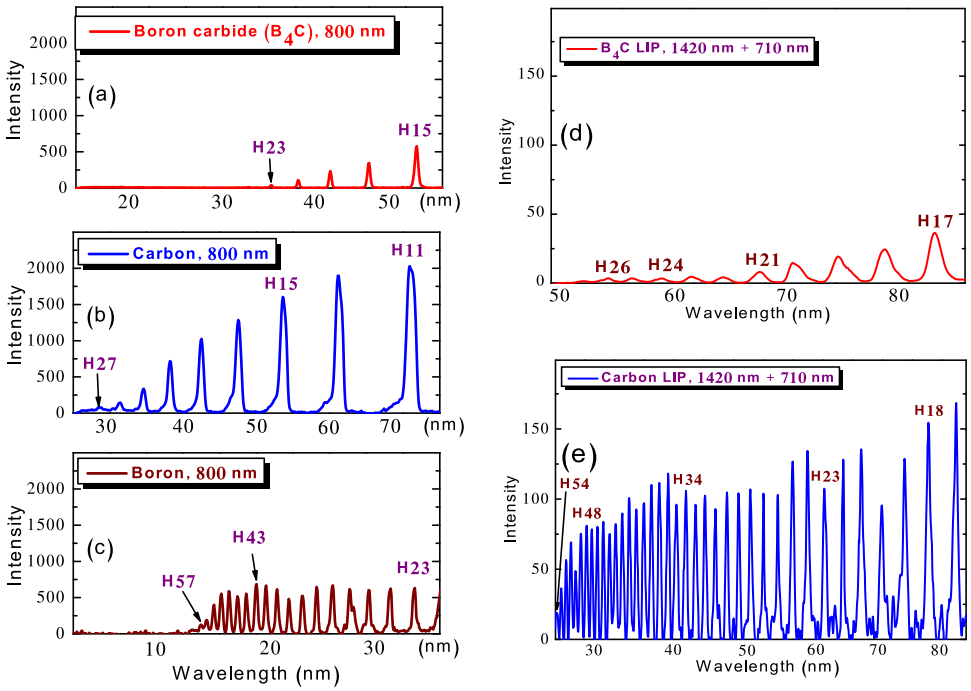

Fig. 2 **a**–**c** Harmonic generation in **a** B_4C LIP, **b** C LIP, and **c** B LIP using 800 nm driving pulses. Harmonic generation in **d** B_4C LIP and **e** C LIP using a two-color pump (1420 + 710 nm)

radiation inside the vacuum chamber allowed the formation of second harmonic emission ($\lambda = 710$ nm), which interacted with the plasma alongside the 1420 nm wave.

The harmonic yield using near IR driving pulses and their second harmonic from the carbon plasma was stronger than the one from the boron carbide plasma (compare the intensities of H18 in Fig. 2d, e). Additionally, the harmonic cutoffs from those plasmas were significantly distinguished from each other (H26 and H54 in the case of B_4C and C LIP, respectively).

The stability of plasma formation and harmonic generation was better in the case of carbon and boron ablation compared to the ablation of the boron carbide target. Despite the exceptional hardness of B_4C, the process of the stable LIP formation lasted during the first 500–1000 shots of the heating pulses. Then the properties of the surface changed due to the formation of crater resulting in worsened plasma characteristics and decreased harmonic yield. In that case, one has to frequently move the target to avoid the decay of harmonic yield. In the case of ablation of softer targets (boron and graphite), the formation of the craters was also observed. However, this process showed lesser influence on HHG in C and B LIP compared to the B_4C LIP. Correspondingly, the process of harmonic generation became rather stable in the cases of C an B LIP compared to the boron carbide plasma. The stable yield of harmonics from boron- and carbon-contained LIP lasted during 5000–10,000 shots, which was one order of magnitude larger compared with the case of boron carbide plasma.

2.2 Increased harmonic cutoff and quasi-phase-matching in Ag plasma compared to Ag_2S plasma

The QPM during HHG in gases and plasmas has been frequently reported using different methods of implementation of this mechanism of harmonic enhancement [53–60]. To create the QPM conditions in LIP, the extended plasma should be transformed into a set of small-sized plasma jets. LIP allows for manipulation of the plasma jet sizes, distance between jets, electron concentration, and other parameters. The most suitable technique here is a modification of the homogeneous extended plasma toward the group of separated plasma jets using the spatially modulated heating beams. It also allows for easy spectral tuning of the maximally enhanced groups of harmonics.

To create extended plasma, the heating pulses were focused using the cylindrical lens. It resulted in the formation of the extended homogeneous LIP (5 mm), which allowed the propagation of the driving pulses through the longer distance inside the plasma compared to the commonly used small-sized LIP produced during the spherical focusing of heating pulses. The sizes of plasma in most reported HHG experiments were varied in the range of 0.3–0.6 mm [61–63].

The growth of the sizes of plasma allows for increase in harmonic yield, which quadratically depends on the length of the medium [74]. However, this increase in conversion efficiency is restricted due to the limitation in the maintenance of the phase-matching conditions in the plasmas containing free electrons. At these conditions, the highest orders of harmonics become strongly suppressed, which leads to a decrease of the harmonic cutoff and conversion efficiency. The separation of homogeneous extended plasma at these conditions onto a group of separated plasma jets can notably resolve the problem of phase mismatching of the higher-order harmonics at the specially chosen conditions of LIP formation.

Multi-slit mask (MSM) was used to create the multi-jet plasmas. In the present experiments, the width of the slits was 0.3 mm with a distance between them 0.3 mm. The MSM was installed between the focusing cylindrical lens and target to divide the 5-mm-long plasma into eight 0.3-mm-long plasma jets with ~0.3-mm separation. The slits of the size of 0.4 mm with a distance between them of 0.4 mm were also used to create six 0.4-mm-long plasma jets with ~0.4 mm separation. As materials for ablation, the silver and silver sulfide targets were used.

Figure 3a shows the raw image of the harmonic spectrum from the 5-mm-long homogeneous silver plasma. The raw images in the set of experiments shown in Fig. 3 are presented for better visual distinction between the harmonic spectra in the case of plateau-like distribution and QPM-induced enhancement of the groups of higher-order harmonics in the case of the variations of plasma morphology. We also show here the plots of these spectral images of harmonics (Fig. 3e, f). TCP (1300 + 650 nm) of both plasmas was used during these studies. The slowly decayed harmonics (from H18 to H43) showed a plateau-like shape of harmonic distribution in the extended LIP. The insertion of MSM on the path of heating beam led to the formation of eight plasma jets on the Ag target. This modification of plasma morphology allowed observation of a significant growth of conversion efficiency for a group of higher-order harmonics centered at H41 (Fig. 3b). These harmonics were barely seen in the case of the extended Ag plasma (Fig. 3a).

The application of extended silver sulfide plasma (Fig. 3c) at optimal conditions of ablation led to generation of weak harmonics. The ratio of intensities of the lower-order harmonics (H18–H23) generated at optimal conditions in Ag and Ag_2S LIP was ~ 7 (compare two red plots in Fig. 3e, f). The application of the QPM technique for Ag_2S plasma by inserting the same MSM used during HHG in silver plasma (8 jets) on the pass of heating pulses did not allow observation of the notably enhanced harmonics in the H35–H48 region (27–38 nm) like in the case of modulated Ag LIP. Because of this another

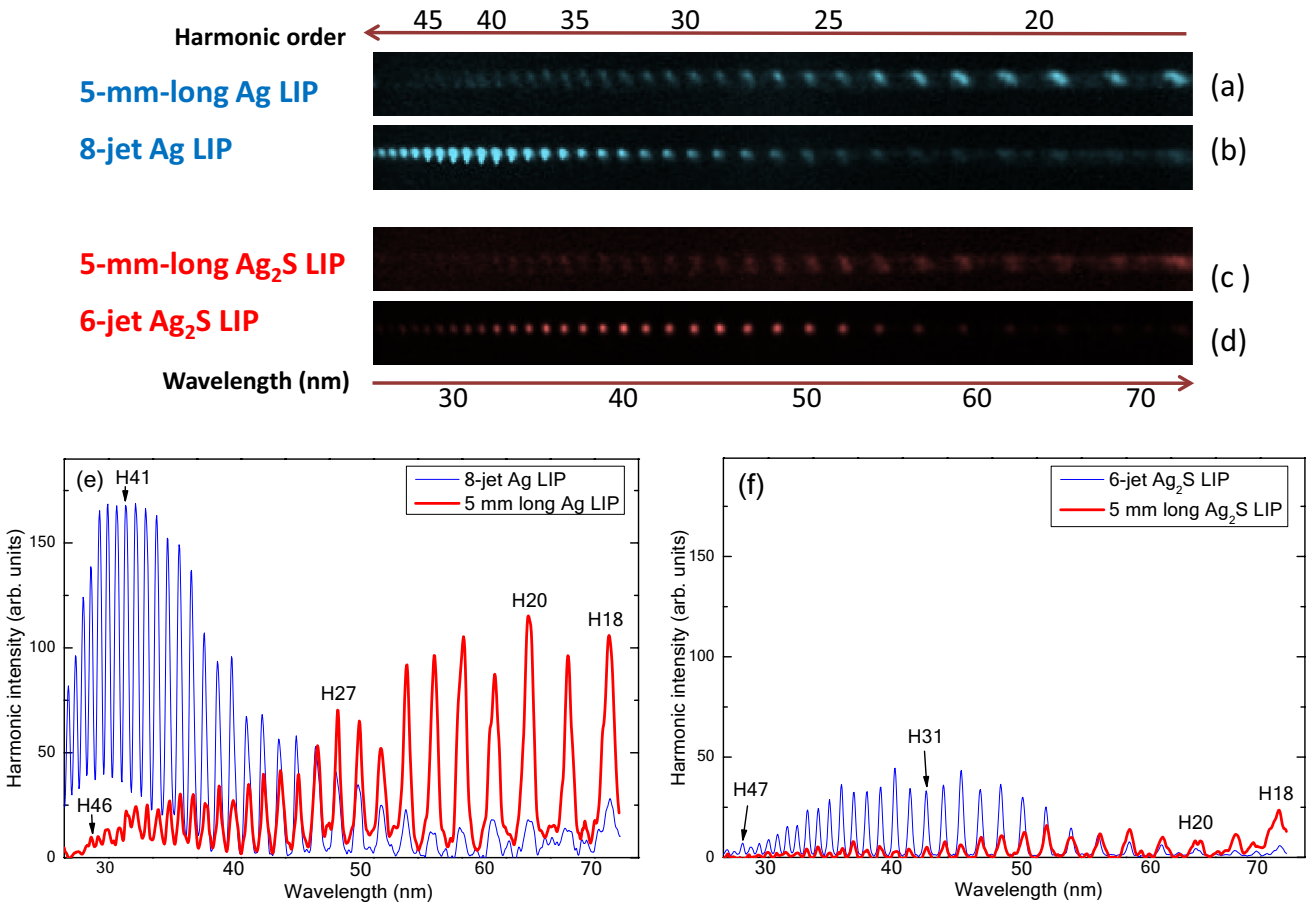

Fig. 3 Raw images of harmonic spectra from **a**, **b** Ag and **c**, **d** Ag_2S plasmas using 1300 + 650 nm two-color pump. Panels (**a**) and (**c**) correspond to the harmonic generation in the extended (5 mm) Ag and Ag_2S plasmas, respectively. Panels (**b**) and (**d**) correspond to the generation of harmonics from 8-jet Ag LIP and 6-jet Ag_2S LIP, respectively. **e** Plots of (**a**) and (**b**) spectra. **f** Plots of (**c**) and (**d**) spectra

MSM with 0.4 mm wide slits was used, which allowed the enhancement of a group of longer-wavelength harmonics (H26–H40, Fig. 3d) in the 6-jet plasma. Like in the case of extended homogeneous plasmas, the maximally enhanced harmonic from the Ag LIP (H41, Fig. 3b) was significantly stronger than the maximally enhanced harmonic from the Ag_2S LIP (H31, Fig. 3d). The ratio of the intensities of those harmonics was ~ 4 (compare two blue plots in Fig. 3e, f). Thus, the formation of the QPM conditions in silver sulfide plasma became less favorable compared to the silver LIP. Among the reasons leading to the worsening of QPM conditions in molecular plasma could be the difficulty in maintenance of a suitable concentration of free electrons in the 0.4-mm-long Ag_2S plasma jets contrary to the case of the multi-jet Ag LIP.

2.3 Decrease of resonance-induced effect of single harmonic enhancement in molecular versus atomic LIP

The resonant amplification of single harmonic in LIP is due to the multiphoton resonance with an exceptionally strong transition of a single-charged ion, which can be shifted due to the Kerr effect toward certain harmonic of the 800-nm-class Ti:sapphire lasers or by using the tunable near-infrared laser sources. This explanation was based solely on the consideration of single-atom response leaving aside the collective processes of optimized phase-matched conditions in the vicinity of ionic transitions.

The altered phase-matching conditions in the region of anomalous dispersion of some transitions can play important role in explaining the phenomenon of single-harmonic amplification and its disappearance under certain conditions. Particularly, the comparison of enhancement factor of H11 in the case of the plasmas comprising the Zn and ZnSe nanoparticles has shown a significant decrease of this parameter in the vicinity of ZnII resonance possessing large oscillator strength (*gf*) in the case of ZnSe plasma [65]. It has been shown that selenides of this metal noticeably reduce the amplification of single harmonic compared to the purely atomic Zn plasma due to a decrease of *gf* of the involved ionic transitions. Stronger ablation of this molecular target did not allow the resonant amplification of single harmonic in ZnSe plasma due to insufficient disintegration of molecules leading to appearance of zinc ions. The mechanism of resonance enhancement of a single harmonic during HHG in indium-contained atomic and molecular plasmas using single-color pump and TCP of ablated species in the case of 800 and 1030 nm lasers was analyzed in Ref. [66]. It was shown that the oxides of this metal notably reduce the enhancement of a single harmonic compared to the atomic plasma due to either shift of the ionic transitions possessing large *gf* out from the wavelength of those harmonics or reduction of *gf* of these transitions.

The above-discussed studies allowed predicting modification of the mechanism of resonant amplification of a single harmonic reported in other atomic plasmas (manganese, tin, tellurium, molybdenum, chromium, and arsenic) being presented in the molecular form. This process can also be reconsidered by comparing the atomic and molecular plasmas containing abovementioned elements, as well as by tuning the wavelength of driving radiation along the resonances responsible for the amplification of harmonics. Below, two species (arsenic- and chromium-contained molecular plasmas) were analyzed from the point of view of the modification of harmonic distribution compared to the arsenic and chromium atomic plasmas.

The experiments using 800 nm laser allowed for demonstration of distinction between the featureless decay of higher-order harmonics generated in GaAs LIP (Fig. 4a, red thick curve) and the appearance of resonance-enhanced H27 generated in As LIP (Fig. 4a, blue thin curve). These studies were carried out using relatively small fluence (2 J cm^{-2}) of the heating pulses ablating GaAs target. The two-fold increase of the fluence of heating pulses allowed observation of the enhanced H27 in the molecular plasma, though the enhancement factor (i.e. ratio of the resonance-enhanced harmonic and the lower-order 25th harmonic) in that case was ~ 1.5, which is notably smaller than the one in the case of pure As LIP (6x, Fig. 4a).

The studies of resonance enhancement in Cr-contained plasmas were carried out using TCP (1236 + 618 nm) scheme. At the optimal conditions of ablation corresponding to the highest harmonic yield the Cr_3C_2 LIP showed a gradual decay of harmonic yield up to H40 (Fig. 4b, red thick curve). The application of Cr LIP increased the yield of all harmonics and extended the cutoff up to the 49th order (Fig. 4b, blue thin curve). The important peculiarity observed during these studies was the appearance of the group of enhanced harmonics in the vicinity of 27 nm. The maximally enhanced harmonic (H44) was stronger than H21.

The origin of the resonance-induced enhancement in chromium plasma in this spectral region was discussed in a few previous studies [45, 67]. It was concluded that some ionic transitions possessing largest *gf* influence the efficiency of harmonic generation thus allowing the enhancement of nearby harmonics. The studies of photoabsorption and photoionization spectra of chromium [68] have demonstrated the presence of strong transitions of CrII, which could be

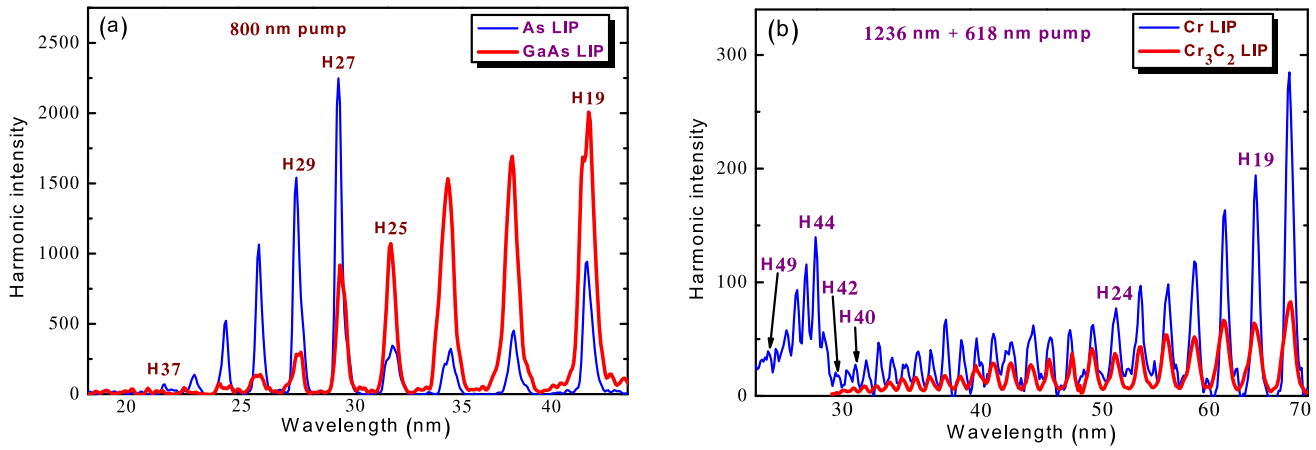

Fig. 4 **a** Harmonic spectra from GaAs LIP (red thick curve) and As LIP (blue thin curve) obtained using the 800 nm driving pulses. **b** Harmonic spectra from Cr_3C_2 LIP (red thick curve) and Cr LIP (blue thin curve) using the 1236 + 618 nm driving pulses.

responsible for the absorption of some harmonic orders in the wavelength region of 29.5–31 nm (see the suppressed H41 and H42 in Fig. 4b in the case of Cr LIP). In the meantime, the strongest ionic transitions $3p \rightarrow 3d$ of CrII in the region 27.6–28.2 nm ($gf = 0.63$ [69]) can enhance the harmonics in the vicinity of those groups of transitions (compare the intensities of H43–H48 and lower-order harmonics, Fig. 4b).

3 Discussion

The aim of these studies was to show a difference in HHG efficiency between the plasmas containing atoms and molecules of those atoms. Because of this we chosen the pairs of plasmas (Ag_2S and Ag, GaAs and As, Cr_3C_2 and Cr, B_4C and C) comprising similar elements. The similar (single-color pump or TCP) experiments were present for almost all pairs. We did not compare the single-color pump of molecular plasma and two-color pump of atomic plasma. By other words, the studies of two plasmas were carried out at similar experimental conditions. The reason to show the single-color-induced and two-color-induced HHG spectra allowed demonstrating the advantages of atomic plasma at different regimes of harmonic generation. This advantage was demonstrated in the case of single-color pump of two plasmas (Fig. 2a–c), TCP (Fig. 2d–e), quasi-phase matching of harmonics (Fig. 3), and resonance enhancement of single harmonic (Fig. 4a–b). Finally, the same can be said about the use of different wavelengths of driving radiation (Figs. 2, 3 and 4). Thus these studies have shown the advantages of atomic plasmas with regard to the molecular plasmas as the media for efficient HHG. This study represents a systematic analysis of the difference of two plasmas from the point of view of various optical processes occurring during HHG.

We showed that the elemental state and composition of plasma play crucial role alerting HHG in this medium. It was demonstrated that, in the case of the plasma comprising molecules, either in neutral or ionized state, almost all parameters of harmonics became affected and decreased or worsened compared with atomic plasma. Meanwhile, once these molecules became disintegrated (for example, from B_4C toward the B and C atoms or ions), the harmonic properties became close to those observed in the case of HHG from ablated boron or carbon plasmas. Our analysis of HHG spectra showed the influence of the composition of the plasmas produced in three studied cases on the spectral distribution and intensity of harmonics. The conversion efficiencies of harmonic generation in the case of atomic and molecular plasmas were $\sim 2.5 \times 10^{-5}$ and $\sim 6 \times 10^{-6}$, respectively. Thus the new approach in analysis of the plasmas as media for HHG is demonstrated. The difference in HHG efficiency between the plasmas containing atoms and molecules of those atoms is reporting for the first time.

Below we address the peculiarities of QPM experiments reported in these studies. One can expect the n^2 growth of harmonic yield for the n-jet configuration compared with the single jet once the phase mismatch becomes suppressed in gases and plasmas [15, 16], which gives the expected growth factor of 64 in the case of eight-jet medium. This estimation was larger than the experimentally measured enhancement factor (~27) for the multi-jet Ag plasma. The expected enhancement factor for the 6-jet plasma is 36, while the experimentally achieved value was 14. This difference in harmonic enhancement in the case of application of different number of jets explains the weaker QPM-enhanced harmonics from 6-jet Ag_2S plasma compared with 8-jet Ag plasma. The maximal enhancement factors were lower compared with value of n^2 at the conditions when absorption processes are turned on, or in the case of unequal properties of the jets, which can arise due to heterogeneous excitation of the extended target.

The theoretical principles of QPM in plasma and role of number of jets on conversion efficiency of maximally enhanced harmonic were discussed in Ref. [60]. The phase mismatch (PMM) problem suppresses high-order harmonic generation of ultrashort laser pulses in both gaseous and plasma media. The PMM is related with the dephasing between the propagated harmonic field and the laser-induced polarization ($\Delta k = qk_1 - k_q$) caused predominantly by the dispersion of medium enhanced by the presence of free electrons. The difference in the velocities of these waves leads to the conditions when, at some distance from the beginning of the medium, the phase shift becomes close to π. After propagation of this distance (coherence length, $L_{coh} = \pi / \Delta k$) the constructive accumulation of harmonic photons reverts to destructive when the newly generated extreme ultraviolet photons being in reverse phase compensate for the earlier generated photons, thus decreasing the harmonic yield. QPM allows diminishing this restriction of harmonic conversion efficiency by different means. Particularly, QPM has been demonstrated by using the multiple gas puffs [15, 16] and multi-jet plasmas [60]. However, in the case of LIP, it remained unclear the separate role in the QPM mechanism of the two groups of free electrons: those generated during target ablation vs. those coming from tunnel ionization in the driving field.

The decrease of heating pulse fluence on the surface of ablating target should lead to a decrease of electron density (due to lesser number of ablation- and tunnel-induced electrons) in the plasma plume followed by the shift of maximally enhanced harmonic toward the shorter-wavelength region. Similarly, one can anticipate that, for the plasma jets of different sizes, the maximally enhanced

harmonics will also be tuned along the XUV spectrum. We observed this behavior of harmonics in the case of 6- and 8-jet plasmas.

Thus, a technique that is generally seen as suitable for overcoming the ionization limitation and that allows one to efficiently generate higher order harmonics is QPM. With the introduction of a spatially periodic structure of suitable periodicity, a wave vector corresponding to this periodicity enters the wave-vector balance, which compensates the wave-vector mismatch [70]. Various schemes to demonstrate or make use of QPM in HHG have been proposed and developed. The idea is that efficient HHG is only enabled in the in-phase region and is suppressed in the out-of-phase region.

4 Conclusions

The high-order harmonic generation in LIP was analyzed from the point of view of the presence of the molecular and atomic components in these media. The harmonic yield using 800 nm and near IR driving pulses and their second harmonics from the carbon and boron plasmas were stronger than those from the boron carbide plasma. Additionally, the harmonic cutoffs from those plasmas were significantly distinguished from each other (H26 and H54 in the case of B_4C and C LIPs, respectively, while using the 1420 + 710 nm driving pulses and H23 and H57 in the case of B_4C and B LIPs, respectively, while using the 800 nm driving pulses).

The extended silver sulfide plasma at optimal conditions of ablation and similar to previous experiments collection of harmonics by CCD camera allowed for generation of the weak harmonics compared to the extended silver LIP. The intensity ratio of the harmonics generated at optimal conditions in extended Ag and Ag_2S LIPs was ~ 4. The maximally enhanced harmonic from the Ag LIP (H41) at QPM conditions was significantly stronger than the maximally enhanced harmonic from the Ag_2S LIP (H31). Thus, the formation of the QPM conditions in the Ag_2S plasma became less favorable compared to the silver LIP.

Finally, the experiments using an 800 nm laser allowed for demonstration of a distinction between the featureless decay of the higher-order harmonics generated in GaAs LIP and the appearance of resonance-enhanced H27 generated in As LIP. Analogous studies of the resonance-induced enhancement in Cr-contained plasmas were carried out using the two-color pump (1236 + 618 nm) scheme. Cr_3C_2 LIP showed a gradual decay of harmonic yield up to H40. The application of Cr LIP increased the yield of all harmonics and extended the cutoff up to the 49th order. The important peculiarity of chromium plasma was the appearance of a group of enhanced harmonics in the vicinity of the strong ionic transitions $3p \rightarrow 3d$ of CrII (27–29 nm).

The conversion efficiencies of harmonic generation in the case of atomic and molecular plasmas were ~ 2.5×10^{-5} and ~ 6×10^{-6}, respectively.

Summing up, the comparison of the molecular and atomic plasmas demonstrated the worsened characteristics of generated coherent extreme ultraviolet radiation in the molecular LIP (weaker conversion efficiency, lower order of generating harmonics, insufficient stability, weakened QPM effect, and absence of the resonance-induced enhancement of single harmonic). Our studies allow concluding that application of simple species like neutral atoms or singly charged atoms as the media for HHG prevails over molecular species comprising the same atoms, which was confirmed during application of different methods of harmonic generation (resonance enhancement of single harmonic, QPM, and two-color pump). Thus, the atomic species are suitable for generation of stronger harmonics. Meanwhile, the application of molecular samples allows analyzing the processes restricting HHG conversion efficiency like modification of energy levels of ionic components in molecular structures compared with the atoms. This shift of transitions in molecules results in decrease of the resonance harmonic effect observed in some atomic plasmas. Similarly, the electron concentration in molecular plasmas may differ from the one in atomic LIPs, which changes the conditions of QPM in the molecular media.

Acknowledgements R.A.G. acknowledges the support of H. Kuroda during these studies.

Author contributions R.A.G.: conceptualization, investigation, formal analysis, writing, and reviewing this paper. B.M.: formal analysis and reviewing of the paper.

Funding State Task for Universities (FZGU-2023–0007).

Data availability The data that support the findings of this study are available on request from the corresponding author.

Declarations

Conflict of interests The authors declare that they has no known competing financial interests or personal relationships that could have appeared to influence the work reported in this paper.

References

1. Y. Akiyama, K. Midorikawa, Y. Matsunawa, Y. Nagata, M. Obara, H. Tashiro, K. Toyoda, Generation of high-order harmonics using laser-produced rare-gas-like ions. Phys. Rev. Lett. **69**, 2176–2179 (1992)
2. S. Kubodera, Y. Nagata, Y. Akiyama, K. Midorikawa, M. Obara, High-order harmonic generation in laser-produced ions. Phys. Rev. A **48**, 4576–4581 (1993)
3. W. Theobald, C. Wulker, F.R. Schafer, B.N. Chichkov, High-order harmonic generation in carbon vapor and low charged plasma. Opt. Commun. **120**, 177–183 (1995)

4. C.-G. Wahlstrom, S. Borgstrom, J. Larsson, S.-G. Pettersson, High-order harmonic generation in laser produced ions using a near-infrared laser. Phys. Rev. A **51**, 585–591 (1995)
5. R.A. Ganeev, V.I. Redkorechev, T. Usmanov, Optical harmonics generation in low-temperature laser produced plasma. Opt. Commun. **135**, 251–256 (1997)
6. A. Krushelnick, W. Tighe, S. Suckewer, Harmonic generation from ions in underdense aluminum and lithium-fluorine plasmas. J. Opt. Soc. Am. A **14**, 1687–1691 (1997)
7. J. Kim, C.M. Kim, H.T. Kim, G.H. Lee, Y.S. Lee, J.Y. Park, D.J. Cho, C.H. Nam, Highly efficient high-harmonic generation in an orthogonally polarized two-color laser field. Phys. Rev. Lett. **94**, 243901 (2005)
8. M. Sayrac, A.A. Kolomenskii, S. Anumula, Y. Boran, N.A. Hart, N. Kaya, J. Strohaber, H.A. Schuessler, Pressure optimization of high harmonic generation in a differentially pumped Ar or H_2 gas jet. Rev. Sci. Instrum. **86**, 043108 (2015)
9. M. Sayrac, A.A. Kolomenskii, J. Strohaber, H.A. Schuessler, High harmonic generation in Ne and H_2 gas mixtures. J. Opt. Soc. Am. B **32**, 2400–2405 (2015)
10. M. Sayrac, A.A. Kolomenskii, H.A. Schuessler, Pressure optimization and phase matching of high harmonics generation in CO_2 and C_2H_2 molecular gases. J. Electron Spectrosc. Related Phenom. **229**, 1–6 (2018)
11. M. Sayrac, A.A. Kolomenskii, J. Dong, H.A. Schuessler, Generation of enhanced even harmonics of fundamental radiation in temporally separated two-color laser fields. J. Electron Spectrosc. Related Phenom. **233**, 22–27 (2019)
12. M. Sayrac, A.A. Kolomenskii, H.A. Schuessler, Pressure dependence of high order harmonic generation in nitrogen molecular gas and atmospheric air. Optik **179**, 994–1000 (2019)
13. M. Sayrac, Generation of coherent extreme ultraviolet radiation in an air gas cell with a high power femtosecond laser system. Opt. Spectrosc. **129**, 825–829 (2021)
14. M. Sayrac, A.A. Kolomenskii, J. Dong, H.A. Schuessler, Generation of even and odd harmonics in the XUV region with controlling the relative delay and polarization of two-color fields. Optik **226**, 165966 (2021)
15. J. Seres, V.S. Yakovlev, E. Seres, C.H. Streli, P. Wobrauschek, C.H. Spielmann, F. Krausz, Coherent superposition of laserdriven soft-X-ray harmonics from successive sources. Nature Phys. **3**, 878–883 (2007)
16. A. Pirri, C. Corsi, M. Bellini, Enhancing the yield of high-order harmonics with an array of gas jets. Phys. Rev. A **78**, 011801 (2008)
17. V. Tosa, V.S. Yakovlev, F. Krausz, Generation of tunable isolated attosecond pulses in multi-jet systems. New J. Phys. **10**, 025016 (2008)
18. Y. Pertot, S. Chen, S.D. Khan, L.B. Elouga Bom, T. Ozaki, Z. Chang, Generation of continuum high-order harmonics from carbon plasma using double optical gating. J. Phys. B **45**, 074017 (2012)
19. S. Haessler, L.B. Elouga Bom, O. Gobert, J.-F. Hergott, F. Lepetit, M. Perdrix, B. Carre, T. Ozaki, P. Salieres, Femtosecond envelope of the high-harmonic emission from ablation plasmas. J. Phys. B **45**, 074012 (2012)
20. M. Kumar, H. Singhal, J.A. Chakera, P.A. Naik, R.A. Khan, P.D. Gupta, Study of the spatial coherence of high order harmonic radiation generated from preformed plasma plumes. J. Appl. Phys. **114**, 033112 (2013)
21. S. Haessler, V. Strelkov, L.B. Elouga Bom, M. Khokhlova, O. Gobert, J.-F. Hergott, F. Lepetit, M. Perdrix, T. Ozaki, P. Salieres, Phase distortions of attosecond pulses produced by resonance-enhanced high harmonic generation. New J. Phys. **15**, 013051 (2013)
22. H. Singhal, P.A. Naik, M. Kumar, J.A. Chakera, P.D. Gupta, Enhanced coherent extreme ultraviolet emission through high order harmonic generation from plasma plumes containing nanoparticles. J. Appl. Phys. **115**, 033104 (2014)
23. N. Rosenthal, G. Marcus, Discriminating between the role of phase matching and that of the single-atom response in resonance plasma-plume high-order harmonic generation. Phys. Rev. Lett. **115**, 133901 (2015)
24. M.A. Fareed, N. Thire, S. Mondal, B.E. Schmidt, F. Legare, T. Ozaki, Efficient generation of sub-100 eV high-order harmonics from carbon molecules using infrared laser pulses. Appl. Phys. Lett. **108**, 124104 (2016)
25. M.A. Fareed, S. Mondal, Y. Pertot, T. Ozaki, Carbon molecules for intense high-order harmonics from laser-ablated graphite plume. J. Phys. B **49**, 035604 (2016)
26. M. Oujja, I. Lopez-Quintas, A. Benítez-Canete, R. de Nalda, M. Castillejo, Harmonic generation by atomic and nanoparticle precursors in a ZnS laser ablation plasma. Appl. Surf. Sci. **392**, 572–580 (2017)
27. M.A. Fareed, V.V. Strelkov, N. Thire, S. Mondal, B.E. Schmidt, F. Legare, T. Ozaki, High-order harmonic generation from the dressed autoionizing states. Nature Commun. **8**, 16061 (2017)
28. M. Wostmann, L. Splitthoff, H. Zacharias, Control of quasi-phase-matching of high-harmonics in a spatially structured plasma. Opt. Express **26**, 14524–14535 (2018)
29. Z. Abdelrahman, M.A. Khohlova, D.J. Walke, T. Witting, A. Zair, V.V. Strelkov, J.P. Marangos, J.W.G. Tisch, Chirp-control of resonant high-order harmonic generation in indium ablation plumes driven by intense few-cycle laser pulses. Opt. Express **26**, 15745–15756 (2018)
30. M.A. Fareed, V.V. Strelkov, M. Singh, N. Thire, S. Mondal, B.E. Schmidt, F. Legare, T. Ozaki, Harmonic generation from neutral manganese atoms in the vicinity of the giant autoionization resonance. Phys. Rev. Lett. **121**, 023201 (2018)
31. M. Kumar, H. Singhal, J.A. Chakera, High order harmonic radiation source for multicolor extreme ultraviolet radiography of carbon plumes. J. Appl. Phys. **125**, 155902 (2019)
32. M. Singh, M.A. Fareed, A. Laramée, E. Isgandarov, T. Ozaki, Intense vortex high-order harmonics generated from laser-ablated plume. Appl. Phys. Lett. **115**, 231105 (2019)
33. J. Liang, Y.H. Lai, W. Fu, Y. Shan, W. Yu, C. Guo, Observation of resonance-enhanced high-order harmonics from direct excitation of metal nanoparticles with femtosecond pulses. Phys. Rev. A **102**, 053117 (2020)
34. S.R. Konda, V.R. Soma, M. Banavoth, R. Ketavath, V. Mottamchetty, Y.H. Lai, W. Li, High harmonic generation from laser-induced plasmas of Ni-doped $CsPbBr_3$ nanocrystals: implications for extreme ultraviolet light sources. ACS Appl. Nano Mater. **4**, 8292–8301 (2021)
35. S.R. Konda, Y.H. Lai, W. Li, Investigation of high harmonic generation from laser ablated plumes of silver. J. Appl. Phys. **130**, 013101 (2021)
36. Y.H. Lai, S.R. Konda, J. Liang, X. Wang, C. Guo, W. Yu, W. Li, Resonance-enhanced high harmonic in metal ions driven by elliptically polarized laser pulses. Opt. Lett. **46**, 2372–2375 (2021)
37. M. Singh, M.A. Fareed, V. Strelkov, A.N. Grum-Grzhimailo, A. Magunov, A. Laramee, F. Legare, T. Ozaki, Intense quasi-monochromatic resonant harmonic generation in the multiphoton ionization regime. Optica **8**, 1122–1125 (2021)
38. J. Liang, Y.H. Lai, W. Fu, C. Guo, W. Li, Distinguishing monomer and nanoparticle contributions to high-harmonic emission from laser-ablated plumes. Opt. Express **29**, 23421–23429 (2021)
39. W. Fu, Y.H. Lai, J. Liang, W. Li, Investigation of high-harmonic cutoff of metal ions driven by near-infrared laser. Opt. Express **30**, 23090–23101 (2022)

40. W. Fu, Y.H. Lai, W. Li, Comparative study of medium length-dependent high-harmonic generation from metal ions. Opt. Express **30**, 47315–47325 (2022)
41. W. Fu, J. Wang, J. Yu, W. Li, Extension of high-order harmonic generation cutoff from laser-ablated tin plasma plumes. Opt. Express **31**, 15553–15563 (2023)
42. M. Singh, M.A. Fareed, V. Birulia, A. Magunov, A.N. Grum-Grzhimailo, P. Lassonde, A. Laramée, R. Marcelino, R.G. Shirinabadi, F. Légaré, T. Ozaki, V. Strelkov, Ultrafast resonant state formation by the coupling of rydberg and dark autoionizing states. Phys. Rev. Lett. **130**, 073201 (2023)
43. J. Mathijssen, Z. Mazzotta, A.M. Heinzerling, K.S.E. Eikema, S. Witte, Material-specific high-order harmonic generation in laser-produced plasmas for varying plasma dynamics. Appl. Phys. B **129**, 91 (2023)
44. R.A. Ganeev, C. Hutchison, A. Zaïr, T. Witting, F. Frank, W.A. Okell, J.W.G. Tisch, J.P. Marangos, Enhancement of high harmonics from plasmas using two-color pump and chirp variation of 1 kHz Ti:sapphire laser pulses. Opt. Express **20**, 90–100 (2012)
45. R.A. Ganeev, T. Witting, C. Hutchison, F. Frank, M. Tudorovskaya, M. Lein, W.A. Okell, A. Zaïr, J.P. Marangos, J.W.G. Tisch, Isolated sub-fs XUV pulse generation in Mn plasma ablation. Opt. Express **20**, 25239–25248 (2012)
46. R.A. Ganeev, C. Hutchison, T. Witting, F. Frank, W.A. Okell, A. Zaïr, S. Weber, P.V. Redkin, D.Y. Lei, T. Roschuk, S.A. Maier, I. López-Quintás, M. Martín, M. Castillejo, J.W.G. Tisch, J.P. Marangos, High-order harmonic generation in graphite plasma plumes using ultrashort laser pulses: a systematic analysis of harmonic radiation and plasma conditions. J. Phys. B **45**, 165402 (2012)
47. S. Patchkovskii, Nuclear dynamics in polyatomic molecules and high-order harmonic generation. Phys. Rev. Lett. **102**, 253602 (2009)
48. K. Yoshii, G. Miyaji, K. Miyazaki, Measurement of molecular rotational temperature in a supersonic gas jet with high-order harmonic generation. Opt. Lett. **34**, 1651–1653 (2009)
49. B. Shan, C. Wang, and Z. Chang, "Near cutoff behaviors of high-order harmonic generation from molecular gases," CLEO/Quantum Electron. Laser Sci. Conf., Technical Digest (Optica Publ. Group), QTuG38 (2003).
50. M. Arias, M. Sanz, M. Oujja, M. Castillejo, Harmonic generation in ablation plasmas of widebandgap semiconductors. Phys. Chem. Chem. Phys. **13**, 10755 (2011)
51. I. Lopez-Quintas, M. Oujja, M. Sanz, M. Martin, R.A. Ganeev, M. Castillejo, Low-order harmonic generation in nanosecond laser ablation plasmas of carbon-containing materials. Appl. Surf. Sci. **278**, 33 (2013)
52. M. Oujja, A. Benítez-Canete, M. Sanz, I. Lopez-Quintas, M. Martín, R. de Nalda, M. Castillejo, Frequency mixing in boron carbide laser ablation plasmas. Appl. Surf. Sci. **336**, 53 (2015)
53. A. Paul, R.A. Bartels, R. Tobey, H. Green, S. Weiman, I.P. Christov, M.M. Murnane, H.C. Kapteyn, S. Backus, Quasi-phase-matched generation of coherent extreme ultraviolet light. Nature **421**, 51–54 (2003)
54. X. Zhang, A.L. Lytle, T. Popmintchev, X. Zhou, H.C. Kaptayn, M.M. Murnane, O. Cohen, Quasi-phase-matching and quantum-path control of high-harmonic generation using counterpropagating light. Nature Phys. **3**, 270–275 (2007)
55. T. Auguste, B. Carrŕe, P. Salières, Quasi-phase-matching of high-order harmonics using a modulated atomic density. Phys. Rev. A **76**, 011802 (2007)
56. A. Nayak, I. Orfanos, I. Makos, M. Dumergue, S. Kühn, E. Skantzakis, B. Bodi, K. Varju, C. Kalpouzos, H.I.B. Banks, A. Emmanouilidou, D. Charalambidis, P. Tzallas, Multiple ionization of argon via multi-XUV-photon absorption induced by 20-GW high-order harmonic laser pulses. Phys. Rev. A **98**, 023426 (2018)
57. A. Willner, F. Tavella, M. Yeung, T. Dzelzainis, C. Kamperidis, M. Bakarezos, D. Adams, M. Schulz, R. Riedel, M.C. Hoffmann, W. Hu, J. Rossbach, M. Drescher, N.A. Papadogiannis, M. Tatarakis, B. Dromey, M. Zepf, Coherent control of high-harmonic generation via dual-gas multijet arrays. Phys. Rev. Lett. **107**, 175002 (2011)
58. X. Wang, M. Chini, Q. Zhang, K. Zhao, Y. Wu, D.A. Telnov, S.-I. Chu, Z. Chang, Mechanism of quasi-phase-matching in a dual-gas multijet array. Phys. Rev. A **86**, 021802 (2012)
59. L.Z. Liu, K. O'Keeffe, S.M. Hooker, Quasi-phase-matching of high-order harmonic generation using multimode polarization beating. Phys. Rev. A **87**, 023810 (2013)
60. R.A. Ganeev, V. Tosa, K. Kovács, M. Suzuki, S. Yoneya, H. Kuroda, Influence of ablated and tunneled electrons on the quasi-phase-matched high-order harmonic generation in laser-produced plasma. Phys. Rev. A **91**, 043823 (2015)
61. R.A. Ganeev, L.B. Elouga Bom, M.C.H. Wong, J.-P. Brichta, V.R. Bhardwaj, P.V. Redkin, T. Ozaki, High-order harmonic generation from C_{60}-rich plasma. Phys. Rev. A **80**, 043808 (2009)
62. R.A. Ganeev, C. Hutchison, M. Castillejo, I. Lopez-Quintas, F. McGrath, D.Y. Lei, J.P. Marangos, Ablation of nanoparticles and efficient harmonic generation using 1 kHz laser. Phys. Rev. A **88**, 033803 (2013)
63. H. Singhal, R.A. Ganeev, P.A. Naik, A.K. Srivastava, A. Singh, R. Chari, R.A. Khan, J.A. Chakera, P.D. Gupta, Study of high-order harmonic generation from nanoparticles. J. Phys. B **43**, 025603 (2010)
64. C.M. Heyl, C.L. Arnold, A. Couairon, A. L'Huillier, Introduction to macroscopic power scaling principles for high-order harmonic generation. J. Phys. B At. Mol. Opt. Phys. **50**, 013001 (2017)
65. R.A. Ganeev, H. Kuroda, High-order harmonics generation in atomic and molecular zinc plasmas. Photonics **8**, 29 (2021)
66. R.A. Ganeev, G.S. Boltaev, V.V. Kim, M. Iqbal, H. Kuroda, A.S. Alnaser, Distinction in resonance properties of the atomic and molecular plasmas used for high-order harmonics generation of ultrafast laser pulses. J. Appl. Phys. **129**, 043103 (2021)
67. V. Strelkov, Role of autoionizing state in resonant high-order harmonic generation and attosecond pulse production. Phys. Rev. Lett. **104**, 123901 (2010)
68. C. McGuinness, M. Martins, P. Wernet, B.F. Sonntag, P. van Kampen, J.-P. Mosnier, E.T. Kennedy, J.T. Costello, Metastable state contributions to the measured 3p photoabsorption spectrum of Cr+ ions in a laser-produced plasma. J. Phys. B **32**, L583–L591 (1999)
69. J.B. West, J.E. Hansen, B. Kristensen, F. Folkmann, H. Kjeldsen, Revised interpretation of the photoionization of Cr+ in the 3p excitation region. J. Phys. B **36**, L327–L333 (2003)
70. Y. Tao, S.J. Goh, H.M.J. Bastiaens, P.J.M. Van der Slot, S.G. Biedron, S.V. Milton, K.-J. Boller, Temporal model for quasi-phase matching in high-order harmonic generation. Opt. Express **25**, 3621–3938 (2017)